

# New Insights into the Molecular Dynamics of Poly-3-hexylthiophene:PCBM Bulk Heterojunction: A Time-of-Flight Quasi-Elastic Neutron Scattering Study

*Anne A. Y. Guilbert<sup>1\*</sup>, Mohamed Zbiri<sup>2\*\*</sup>, Maud V. C. Jenart<sup>3</sup>, Christian B. Nielsen<sup>3</sup>, Jenny Nelson<sup>1</sup>*

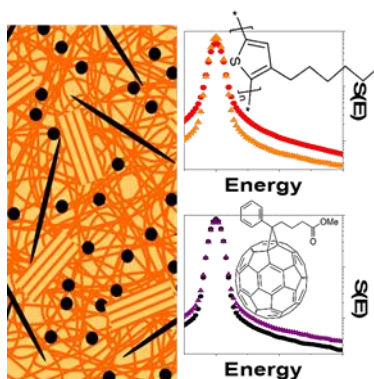
<sup>1</sup> Centre for Plastic Electronics and Department of Physics, Blackett Laboratory, Imperial College London, London SW7 2AZ, United Kingdom

<sup>2</sup> Institut Laue-Langevin, 71 avenue des Martyrs, Grenoble Cedex 9, FR 38042.

<sup>3</sup> Centre for Plastic Electronics and Department of Chemistry, Imperial College London, UK

**ABSTRACT** The molecular dynamics of organic semiconductor blend layers are likely to affect the optoelectronic properties and the performance of devices such as solar cells. We study the dynamics (5 - 50 ps) of the poly(3-hexylthiophene) (P3HT): phenyl-C61-butyric acid methyl ester (PCBM) blend by time-of-flight quasi-elastic neutron scattering, at temperatures in the range 250 – 360 K, thus spanning the glass transition temperature region of the polymer and the operation temperature of an OPV device. The behavior of the QENS signal provides evidence for the vitrification of P3HT upon blending, especially above the glass transition temperature, and the plasticization of PCBM by P3HT, both dynamics occurring on the picosecond time scale.

## TOC GRAPHICS



Organic photovoltaic (OPV) devices have attracted a keen interest over the past decade for their potential low-cost, light-weight, flexibility and ease of use and processing. In contrast to inorganic solar cells, the photocurrent generation results from two consecutive processes

consisting of the dissociation of photogenerated excitons into free charges at a donor:acceptor (D:A) interface, followed by the transport of those free charges to the relevant electrodes. Transient optical spectroscopy has been used extensively to probe the radiative decay of the different states on time scales from a few femtoseconds up to milliseconds to infer the mechanisms of such processes.<sup>1</sup> If processes occurring at both time scales are not fully understood yet, there is some evidence that the separation of excitons into free charges occurs on tens of fs to ps time scales.<sup>2</sup>

The influence of the microstructure of the D-A blend on the efficiency of such processes has been highlighted.<sup>3</sup> However, only a few reports exist on the effect of both polymer and fullerene dynamics on these processes.<sup>4</sup> The impact of adding a fullerene derivative on the polymer dynamics has been inferred by showing an increase of the glass transition temperature as a function of the fullerene addition, using differential scanning calorimetry.<sup>5</sup> However, extensive studies on non-conjugated polymers highlight the occurrence of various dynamical behaviors within the broad time scale of fs to ms. The latter reflect different dynamics ranging from vibrations of atoms, through rotations of the side chain groups (ps to ns), to backbone motions at longer time scales (> ns). Therefore, these dynamics are likely to impact the photoelectric processes.

Furthermore, under practical operational conditions, OPV devices operate within a temperature range from ambient temperature up to 360 K (at a maximum sun exposure).<sup>6</sup> Therefore, studying the temperature-dependence of such dynamics is of considerable importance.

Recently, a few computational studies attempted to capture the impact of the D-A microstructure by using molecular dynamic simulations as an initial structure to study charge separation.<sup>7</sup>

However, the simulated structures were not validated experimentally, neither were the dynamics studied. Reducing the dimensionality from atom coordinates to few degrees of freedom is needed to carry on more detailed quantum chemistry calculations from those initial structures, and is a demanding task.

Paternó *et al.* studied the dynamics of the hydrogenated poly(3-hexylthiophene) (P3HT):phenyl-C61-butyric acid methyl ester (PCBM) blend, using different solvents, within a time window of about 10 to 470 ps. They reported a change in the dynamics occurring around 285 K, corresponding to the temperature range of the glass transition of P3HT reported in literature. They noted a frustration of the polymer dynamics when the fullerene was added, but only at an elevated temperature of 435 K, while no noticeable difference in dynamics was observed at 340 K, as a function of the solvent.<sup>8</sup> In the same context of probing dynamics, Etampawala *et al.* studied the polymer dynamics in blends with lower fullerene concentrations (up to 10%), and in a time window of about 100 ps to 2 ns.<sup>9</sup>

In this letter, we study the dynamics of the well-known P3HT:PCBM blend at 1:1 weight ratio by quasi-elastic neutron scattering (QENS) in a time window of about 5 to 50 ps, and within the temperature range 250 K to 360 K. This time domain, directly relevant for charge carrier separation processes, offers deeper and complementary insights into the fast component of the dynamics of the P3HT-PCBM blend. The selected temperature domain covers the glass transition of P3HT, as well as the temperature regime of organic solar cells under operational conditions. Further, as an interesting novelty with respect to previous related works,<sup>8-9</sup> we study the fully deuterated P3HT, and partially deuterated PCBM (only the phenyl ring is deuterated for this study) and their blends with fully hydrogenated polymer and fullerene. This allows to reduce the incoherent scattering of one or both of the materials enabling signal discrimination from the

two components of the blend (see Tables S1 and S2 in Supporting Information), and therefore leading to the specific characterization of PCBM dynamics in the polymer matrix. In the following, hydrogenated and (partially) deuterated P3HT/PCBM will be indicated by a prefix h- and d-, respectively.

The Q-averaged dynamic structure factor  $S(E)$ , at 250 and 360 K, is plotted in Figure 1. A base temperature (10 K) measurement served for an energy resolution purpose. Figure 1 a-b, and c-d, show the impact of blending on the polymer dynamics, and the fullerene dynamics, respectively. At 250 K, upon blending, a tiny difference is observed for the polymer dynamics, while no noticeable effect is distinguishable for the fullerene. However, at 360 K, above the glass transition of the polymer, the dynamics of P3HT becomes frustrated due to blending. This is reflected by the intensity increase of the elastic peak, and the narrowing of the quasi-elastic signal. A smaller difference is observed at 360 K for PCBM. Interestingly, PCBM dynamics is enhanced at 360 K as the elastic peak decreases and the quasi-elastic signal broadens.

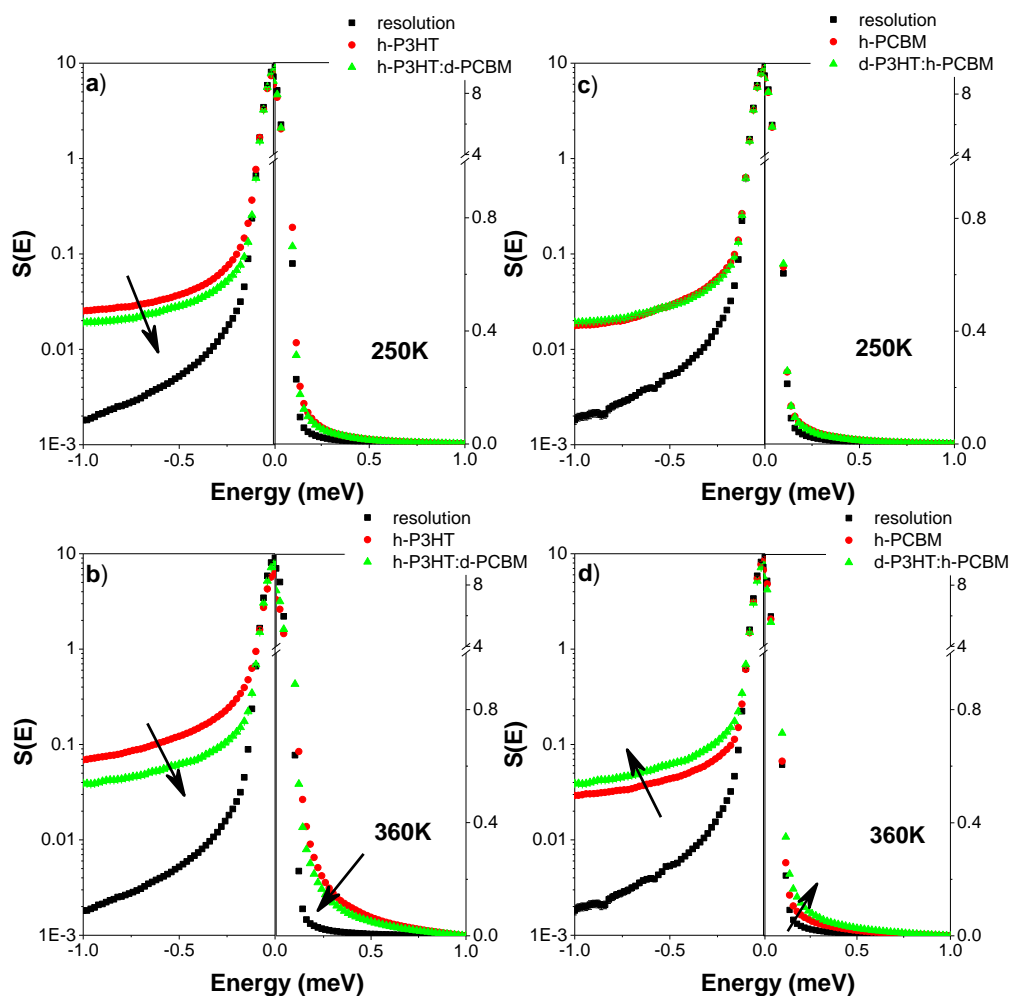


Figure 1. Q-averaged dynamic structure factors for (a and b) h-P3HT, h-P3HT:d-PCBM, (c and d) h-PCBM, and d-P3HT:h-PCBM, at 250 K (a and c) and 360 K (b and d). In each case the black dotted spectrum corresponds to data collected at 10 K, to represent the resolution function of the instrument. In each case, the right panel displays the background corrected QENS signal.

Further, we derived the intermediate scattering functions,  $I(t, Q)$ , by Fourier transforming the background corrected QENS signals and deconvoluting the instrumental resolution (the underlying methodology presently used can be found in the Supporting Information).

Intermediate scattering functions are displayed, at 250 and 360 K, for h-P3HT in Figure 2a, h-P3HT:d-PCBM in Figure 2b, h-PCBM in Figure 2c and d-P3HT:h-PCBM in Figure 2d for different Q values.

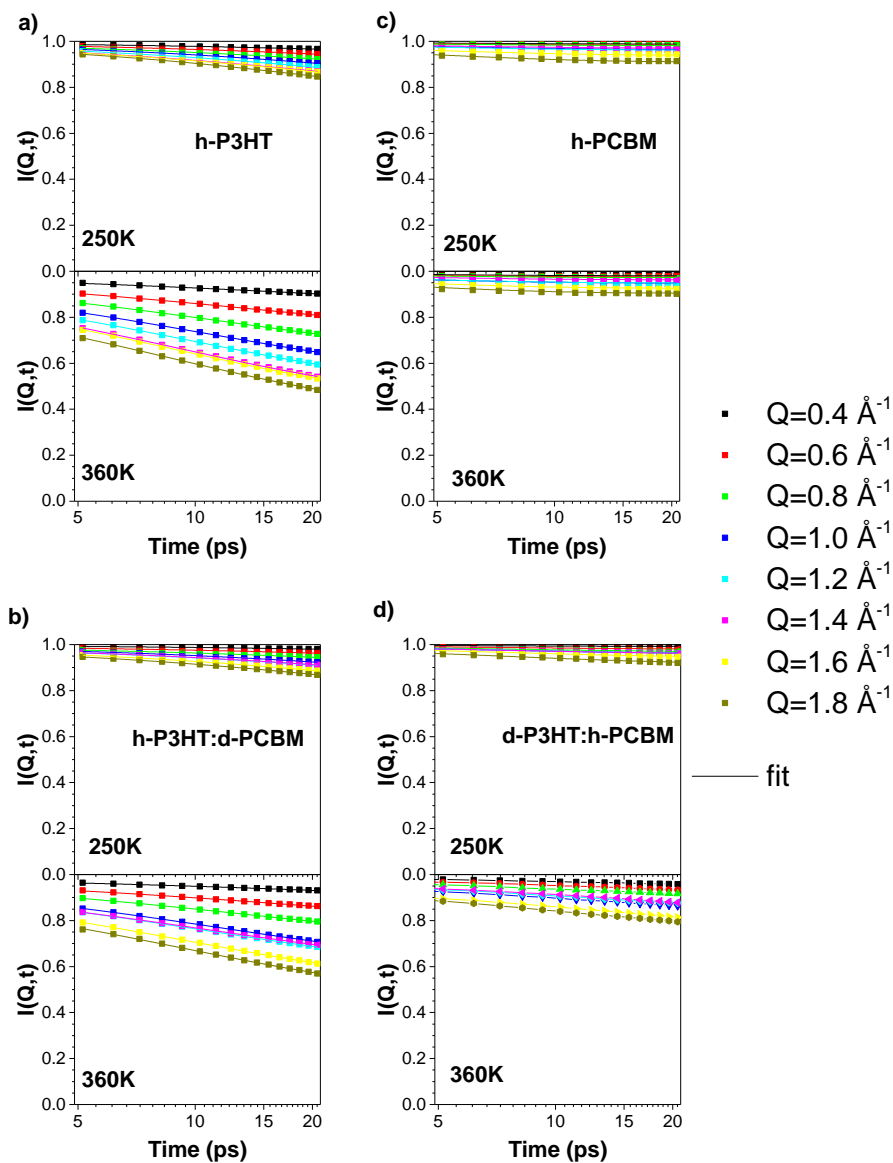


Figure 2. Q-dependence of the intermediate scattering functions (scattered points), at 250 and 360 K, for (a) h-P3HT, (b) h-P3HT:d-PCBM, (c) h-PCBM, and (d) d-P3HT:h-PCBM. The lines are fits using a stretched exponential model.<sup>10-11</sup>

Overall, a broad stretching of  $I(t, Q)$  is observed over the different  $Q$  values for h-P3HT and h-P3HT:d-PCBM. At 250 K, the values of  $I(t, Q)$  vary between 0.8 and 1.0, while at 360 K,  $I(t, Q)$  functions show a decrease within the range 0.4 - 1.0. This is due to the decrease of the elastic contribution and indicates the activation of further dynamical modes. In contrast, almost no stretching is observed at both temperatures for h-PCBM. Interestingly, d-P3HT:h-PCBM exhibits the same behavior as h-PCBM at 250 K while d-P3HT:h-PCBM adopts an intermediate behavior between h-P3HT:d-PCBM at 250 and 360K. In order to better understand these behaviors, we performed a fit of the intermediate scattering functions using the following stretched exponential model:

$$I(t, Q) = (1 - EISF(Q)) * \exp\left(-\left(\frac{t}{\tau(Q)}\right)^\beta\right) + EISF(Q) \quad \text{Equation 1}$$

where  $EISF(Q)$  is the elastic incoherent structure factor,  $\tau$  is the  $Q$ -dependent relaxation time of the measured dynamics, and  $\beta$  is the stretched exponent.<sup>10-11</sup>

Within the available time window, this experiment is unlikely to capture the (slow) relaxation of the backbones, or the complete reorientation of the fullerene but likely to measure the reorientation of the aliphatic side chains of both polymer and fullerene. In the case of localized motions such as side chain end-group rotations,  $\tau$  is expected to be  $Q$  independent. In the case of diffusive jumps for the reorientation of the side chains,  $\langle\tau\rangle$  is expected to be proportional to  $Q^2$  at low  $Q$ s and plateau around  $\tau_0^{-1}$  at high  $Q$ s,  $\tau_0$  being the residence time before jump. Given the restricted window and the number of fitting parameters, it is hard to differentiate between a change in  $EISF(Q)$  and a change in  $\tau(Q)$ . Therefore, we adopt two different fitting strategies.

In the first one, we assume that  $EISF(Q) = REISF(Q) - A$  where  $REISF(Q) \approx I(Q, t = \tau_{res})$  is the resolution dependent elastic incoherent structure factor.  $A$  takes into account the excess of elastic fraction due to apparently localized particles and is assumed  $Q$  independent.  $REISF(Q)$  can be calculated by  $\frac{S(Q, E=0 \text{ meV}, T)}{S(Q, E=0 \text{ meV}, T=10K)}$ , providing that the QENS signal have been corrected for the background and their area normalized to one.  $\langle \tau \rangle^{-1} = \frac{\beta}{\Gamma(1/\beta)}$  is plotted as function of  $Q^2$  in Figure 3 a for samples containing h-P3HT and in Figure 3 b for blends with d-P3HT. It was not possible to fit the data with this model for neat h-PCBM and d-PCBM since.

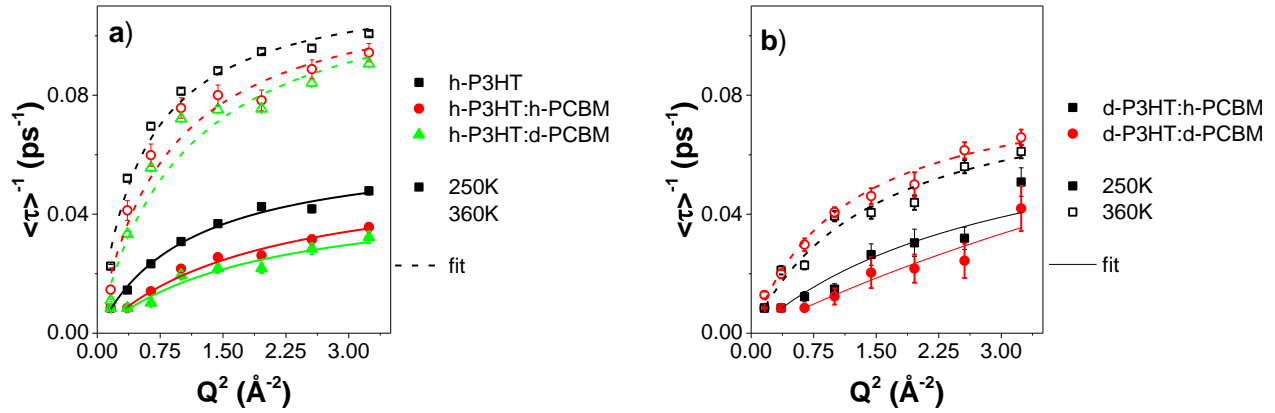


Figure 3.  $\langle \tau \rangle^{-1}$  extracted from the stretched exponential fit (scattered points), at 250 K and 360 K, as a function of  $Q$ , for (a) h-P3HT, h-P3HT:h-PCBM, h-P3HT:d-PCBM and for (b) d-P3HT:h-PCBM, d-P3HT:d-PCBM.

Jump diffusion behavior is observed for all samples except h- and d-PCBM. For blends with at low temperature, a plateau at low  $Q$ s is observed indicative of confinement within a sphere of radius around 8-10 Å. The side chains state as well as PCBM molecules within the amorphous mixture are most likely confined in solid-state by the backbones of the polymer. We performed a fit of  $\langle \tau \rangle (Q)^{-1}$  using the following equation:

$$\langle \tau \rangle (Q)^{-1} = \frac{DQ^2}{1+DQ^2\tau_0} \quad \text{Equation 2}$$

where  $D$  is the diffusion coefficient and  $\tau_0$  the residence time. We find diffusion coefficients of the order of  $0.05 \text{ \AA}^2.\text{ps}^{-1}$  for all the samples at 250 K and for the blends with d-P3HT at 360K. For h-P3HT and its blend, the diffusion coefficient increases to about  $0.15 \text{ \AA}^2.\text{ps}^{-1}$  at 360K. The residence time is about 20 ps for all the samples at 250K and decreases to about 10 ps at 360K (see Table S3).

In the second fitting strategy,  $\tau$  and  $\beta$  are kept  $Q$ -independent, assuming localized motions, while  $\text{EISF}(Q)$  is allowed to vary freely.  $\text{EISF}(Q)$  are plotted for the two fitting strategies in Figure S3 in Supporting Information illustrating the high dependency of the fitting parameters. The probability distribution functions,  $P(E, \tau, \beta)$ ,<sup>12</sup> corresponding to the stretched exponential fits are plotted for samples containing h-P3HT in Figure 4 a and for neat fullerene samples and blends with d-P3HT in Figure 4 b.

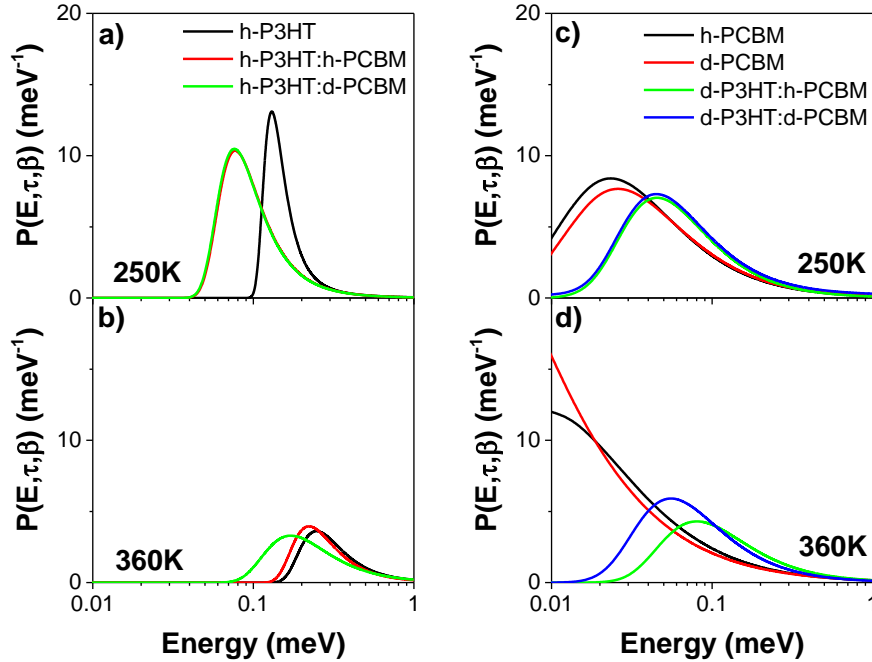


Figure 4. Probability distribution functions  $P(E, \tau, \beta)$  of the relaxation times as the function of the energy for the h-P3HT, h-P3HT:h-PCBM and h-P3HT:d-PCBM (a and b) and for h-PCBM, d-PCBM, d-P3HT:h-PCBM and d-P3HT:d-PCBM (c and d) at 250 K (a and c) and 360 K (b and d).

Two types of dynamics can clearly be distinguished in Figure 4. The first one relates to a narrow probability distribution at high energies that broadens at 360 K for the polymer, and the second corresponds to a broader distribution at low energies for PCBM. Upon blending, the polymer probability distribution is slightly broadened and shifted to lower energies while the opposite trend is observed for PCBM. This is indicative of the frustration of the polymer dynamics. Some small differences are observed between hydrogenated and deuterated samples i.e. h-P3HT:h-PCBM and h-P3HT:d-PCBM samples. This can be due to a number of factors including the difference of mass, possible difference of miscibility and crystallinity.

As a conclusion, we observed the vitrification of P3HT upon blending especially above the glass transition of the polymer, while the plasticization of PCBM by P3HT is also evidenced. Studying in details the dynamics of the blend on 5 - 50 ps time scale reveals a rich temperature-dependent dynamics of the side chain of both components. A forthcoming paper will be dedicated to unravel this complex dynamical behavior by using molecular dynamics simulations.

Side chains are mainly insulators and thus, the appearance of heterogeneous dynamics of these side chains on time scale relevant for charge generation is likely to modulate intermolecular electronic couplings between polymer and fullerene due to screening effects. These dynamics are drastically impacted by temperature as shown in this study, especially for low glass transition polymer such as P3HT and are likely to play an important role in solar cell degradation.

## Experimental method

PCBM and d-PCBM ([6,6]-Pentadeuterophenyl-C61-butyric acid methyl ester) were supplied by Solenne BV. P3HT was obtained from Merck Chemicals (RR = 94.7%, Mn = 19.5 kg/mol, Mw = 34.1 kg/mol, PD= 1.74). The fully deuterated polymer, d-P3HT, was prepared according to a literature procedure,<sup>13</sup> and was obtained with a number-average molecular weight of 30 kg/mol and a polydispersity of 1.5 (see Supporting Information).

The as-received materials were dissolved in chloroform (40 mg/mL) and drop-cast on a glass slide on a hot plate at 60 °C for an hour. The drop-cast films were further dried in a vacuum oven for an hour. The films were then scratched and reduce to powder. The obtained powder was then pressed at 100 °C at an applied force of 10 kN.m<sup>-2</sup> for 15 minutes using a Rondol Technology hot press. Resulting films were of a thickness of about 0.2 mm.<sup>14</sup> PCBM was measured in the powder form obtained after scratching drop-cast film due to the poor quality of the films when pressed. However, we measured the other samples in both powder and film form and no difference in dynamics was observed e.g between the pressed film and powder h-P3HT:h-PCBM samples as evidenced by the QENS dynamic structure factors in Figure S4 in Supporting Information.

The QENS measurements on hydrogenated and deuterated P3HT-PCBM blends (prepared as described above), as well as on individual P3HT and PCBM were performed on the direct-geometry cold neutron, time-of-flight time-focusing spectrometer IN6 at the Institut Laue Langevin (Grenoble, France). The small sample thickness of 0.2 mm is relevant to the minimization of effects like multiple scattering and absorption. Data were collected at 10, 250 and 360 K. The former served as a base temperature for an energy resolution purpose, whereas

the two other temperatures were chosen in such way to cover the glass transition temperature region of the polymer. An incident neutron wavelength  $\lambda_i=5.12 \text{ \AA}$  ( $E_i=3.12 \text{ meV}$ ) was used, offering an energy resolution at the elastic line of  $\sim 0.07 \text{ meV}$ . Standard corrections including detector efficiency calibration and background subtraction were performed. A standard vanadium sample was used to calibrate the detectors. The data analysis was done using ILL software tools. At the used wavelength, the IN6 angular detector coverage ( $\sim 10 - 114^\circ$ ) corresponds to a Q-range of  $\sim 0.2 - 2.1 \text{ \AA}^{-1}$ . Different data sets were extracted either by performing a full Q-average in the (Q,E) space to get the scattering function  $S(E,T)$ , or by considering Q-slices to study the  $S(Q,E,T)$ .

#### ASSOCIATED CONTENT

#### AUTHOR INFORMATION

##### **Corresponding Author**

\*Email: [a.guilbert09@imperial.ac.uk](mailto:a.guilbert09@imperial.ac.uk)

Phone: +(44) (0)2075947563

\*\*Email: [zbiri@ill.fr](mailto:zbiri@ill.fr)

Phone: +33 (0)4 76 20 7803

##### **Notes**

The authors declare no competing financial interests.

#### ACKNOWLEDGMENT

The Institut Laue-Langevin (ILL) facility, Grenoble, France, is acknowledged for providing beam time on the IN6 spectrometer. The authors acknowledge Natalie Stingelin for providing the hot

press, Alberto Scaccabarozzi and Astrid Armgarth from the department of Materials Science (Imperial College London) for fruitful discussions about processing and Alex Sieval from Solenne BV for discussion about deuterated fullerenes. A.G. and J.N. acknowledge the EPSRC Supergen hub (EP/J017361 and EP/M014797/1) and EPSRC grants (EP/K029843/1 and EP/K030671/1). M.J. and C.N. acknowledge financial support from EC FP7 Project SC2 (610115) and EC H2020 Project SOLEDlight (643791).

### **Supporting Information.**

Details on the calculation of the intermediate scattering functions, results of the stretched exponential fits, details of the synthesis of deuterated P3HT, and a comparison between pressed and non-pressed samples are available in the Supporting Information.

### REFERENCES

- (1) Dimitrov, S. D.; Durrant, J. R. Materials Design Considerations for Charge Generation in Organic Solar Cells. *Chem. Mater.*, **2014**, *26*, 616–630.
- (2) Gao, F.; Inganäs, O. Charge Generation in Polymer-Fullerene Bulk-Heterojunction Solar Cells. *Phys. Chem. Chem. Phys.*, **2014**, *16*, 20291–20304.
- (3) Etzold, F.; Howard, I. A.; Forler, N.; Cho, D. M.; Meister, M.; Mangold, H.; Laquai, F. The Effect of Solvent Additives on Morphology and Excited-State Dynamics in PCPDTBT:PCBM Photovoltaic Blends. *J. Am. Chem. Soc.*, **2012**, *134*, 10569–10583.
- (4) Obrzut, J.; Page, K. A. Electrical Conductivity and Relaxation in Poly(3-hexylthiophene). *Phys. Rev. B*, **2009**, *80*, 195211.

- (5) Zhao, J.; Swinnen, A.; Van Assche, G.; Manca, J.; Vanderzande, D.; Van Mele, B. Phase Diagram of P3HT/PCBM Blends and its Implication for the Stability of Morphology. *J. Phys. Chem. B*, **2009**, *113*, 1587–1591.
- (6) Emmott, C. J. M.; Moia, D.; Sandwell, P.; Ekins-Daukes, N.; Hösel, M.; Lukoschek, L.; Nelson, In-Situ, Long-Term Operational Stability of Organic Photovoltaics for Off-Grid Applications in Africa. *Sol. Energy Mater. Sol. Cells*, **2016**, *149*, 284–293.
- (7) Castet, F.; D'Avino, G.; Muccioli, L.; Cornil, J.; Beljonne, D. Charge Separation Energetics at Organic Heterojunctions: on the Role of Structural and Electrostatic Disorder. *Phys. Chem. Chem. Phys.*, **2014**, *16*, 20279–20290.
- (8) Paternó, G.; Cacialli, F.; García-Sakai, V. Structural and Dynamical Characterization of P3HT/PCBM Blends. *Chem. Phys.*, **2013**, *427*, 142–146.
- (9) Etampawala, T.; Ratnaweera, D.; Morgan, B.; Diallo, S.; Mamontov, E.; Dadmun, M. Monitoring the Dynamics of Miscible P3HT:PCBM Blends: A Quasi Elastic Neutron Scattering Study of Organic Photovoltaic Active Layers. *Polymer*, **2015**, *61*, 155–162.
- (10) Williams, G.; Watts, D. C. Non-Symmetrical Dielectric Relaxation Behaviour arising from a Simple Empirical Decay Function. *Trans. Faraday Soc.*, **1970**, *66*, 80.
- (11) Gerstl, C.; Schneider, G. J.; Fuxman, A.; Zamponi, M.; Frick, B.; Seydel, T.; Arbe, A. Quasielastic Neutron Scattering Study on the Dynamics of Poly(alkylene oxide)s. *Macromolecules*, **2012**, *45*, 4394–4405.
- (12) Berberan-Santos, M. N.; Bodunov, E. N.; Valeur, B. Mathematical Functions for the Analysis of Luminescence Decays with underlying Distributions 1. Kohlrausch Decay Function (Stretched Exponential). *Chem. Phys.*, **2005**, *315*, 171–182.

(13) Tournebize, A.; Bussière, P.-O., Rivaton, A., Gardette, J.-L., Medlej, H., Hiorns, R. C., Norrman, K. New Insights into the Mechanisms of Photodegradation/Stabilization of P3HT:PCBM Active Layers Using Poly(3-hexyl- d 13 -Thiophene). *Chem. Mater.*, **2013**, *25*, 4522–4528.

(14) Baklar, M. A.; Koch, F.; Kumar, A.; Buchaca Domingo, E.; Campoy-Quiles, M.; Feldman, K.; Yu, L.; Wobkenberg, P.; Ball, J.; Wilson, R. M. *et al.*, N. Solid-State Processing of Organic Semiconductors. *Adv. Mater.* **2010**, *22*, 3942-3947.